

# Supersaturation Fluctuations from Scalar Transport in Moist Rayleigh-Bénard Convection: One-Dimensional-Turbulence Simulation

Kamal Kant Chandrakar <sup>1</sup>, Will Cantrell <sup>1</sup>, Steven Krueger <sup>2</sup>, Raymond A. Shaw <sup>1</sup>, and Scott Wunsch <sup>3</sup>

<sup>1</sup>Department of Physics, Michigan Technological University <sup>2</sup>Department of Atmospheric Sciences, University of Utah <sup>3</sup>Applied Physics Laboratory, Johns Hopkins University

## Introduction

A careful characterization of moisture fluxes and supersaturation statistics in atmospheric convection is significant for cloud microphysical processes and dynamics. The small-scale supersaturation fluctuation could be an important mechanism for droplet size-distribution broadening [1]. In an idealized sense, atmospheric boundary-layer convection is equivalent to Rayleigh-Bénard convection [2, 3]. Here, continuous plume eruption from boundaries transports heat and moisture and produces the mixed layer [4]. The presence of multiple driving scalars (water vapor and temperature), with slightly different diffusivities, adds to the degree of complexity. Additionally, in the supersaturation statistics, a nonlinear coupling between water-vapor and temperature fields makes the problem intriguing. Important parameters for this problem are [5]:

$$Ra_{moist} \approx \frac{g\Delta TH^3}{T_0\nu D_t} + \frac{g\epsilon\Delta q_v H^3}{\nu D_t}, \quad Pr \equiv \frac{\nu}{D_t}, \quad \text{and} \quad Sc \equiv \frac{\nu}{D_v}.$$

## Numerical Approach

We approach this problem using an idealized, one-dimensional-turbulence (ODT) model that faithfully represents the processes of advection and diffusion in turbulent convection, including fully-resolved boundary layers [6]. The range of Rayleigh number  $2.05 \times 10^8 \leq Ra_{moist} \leq 2.75 \times 10^9$  covered in simulations is relevant to the  $\Pi$ -chamber. In order to understand the relative roles of the two diffusivities, we use the following four combinations.

- Actual  $D_v$  and  $D_t$ : actual diffusivities for the water vapor and thermal fields at 283 K ( $D_v/D_t = 1.16$ ).
- $D_v = D_t$ :  $D_v$  = the actual thermal diffusivity ( $D_v/D_t = 1$ ).
- $4 \times D_v$ :  $D_v$  = four times the actual value, and  $D_t$  = same as the actual value ( $D_v/D_t = 4.63$ ).
- $4 \times D_t$ :  $D_v$  = same as the actual value, and  $D_t$  = four times the actual value ( $D_v/D_t = 0.29$ ).

## Boundary Fluxes

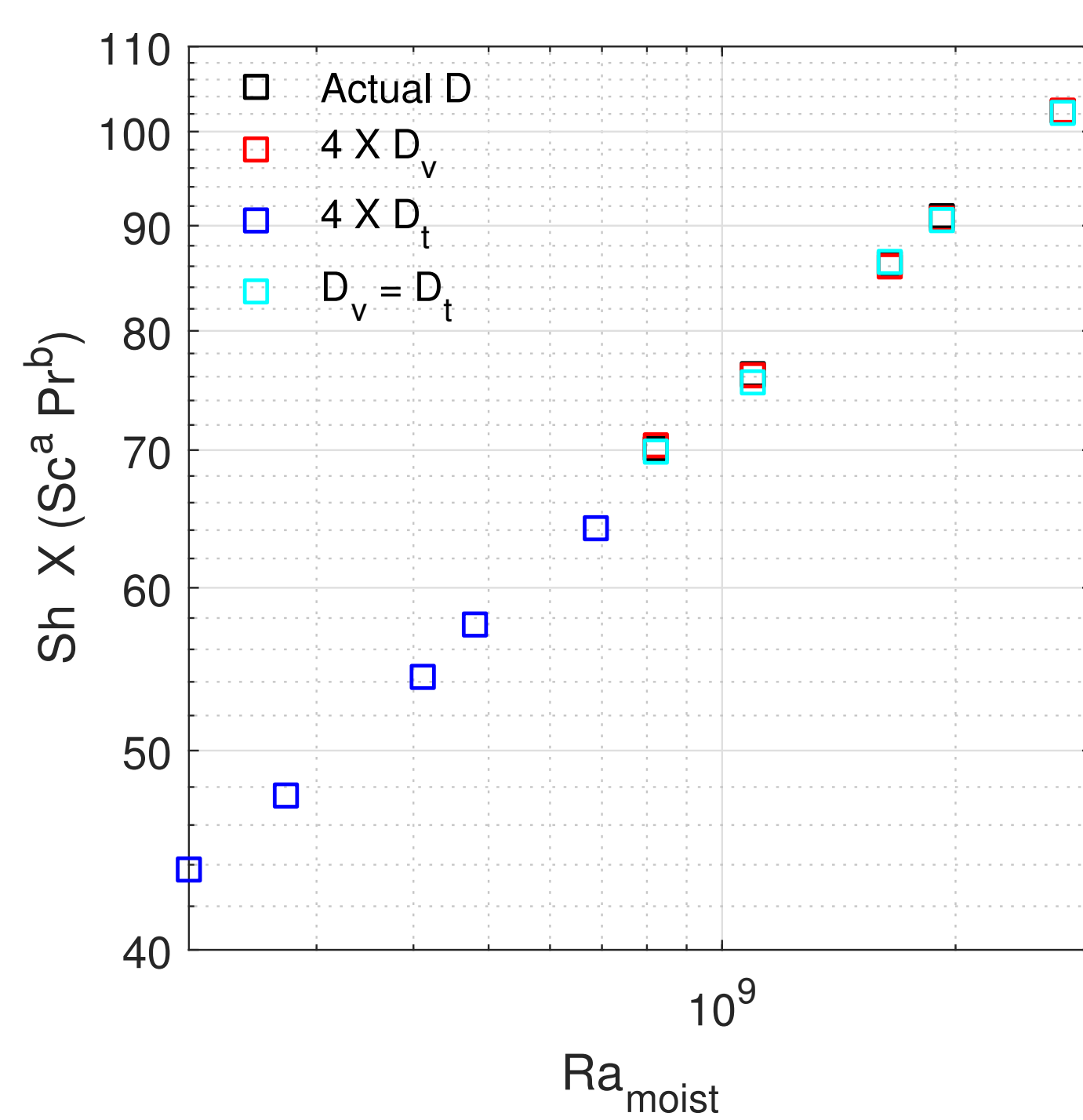


Figure 1: Variation of the scalar fluxes of water vapor ( $Sh$ ) with moist Rayleigh number ( $Ra_{moist}$ ). Fitting of the scaled  $Sh$  data produce  $Ra_{moist}$  exponents around  $0.328 \pm 0.006$ .

## Supersaturation Fluctuations

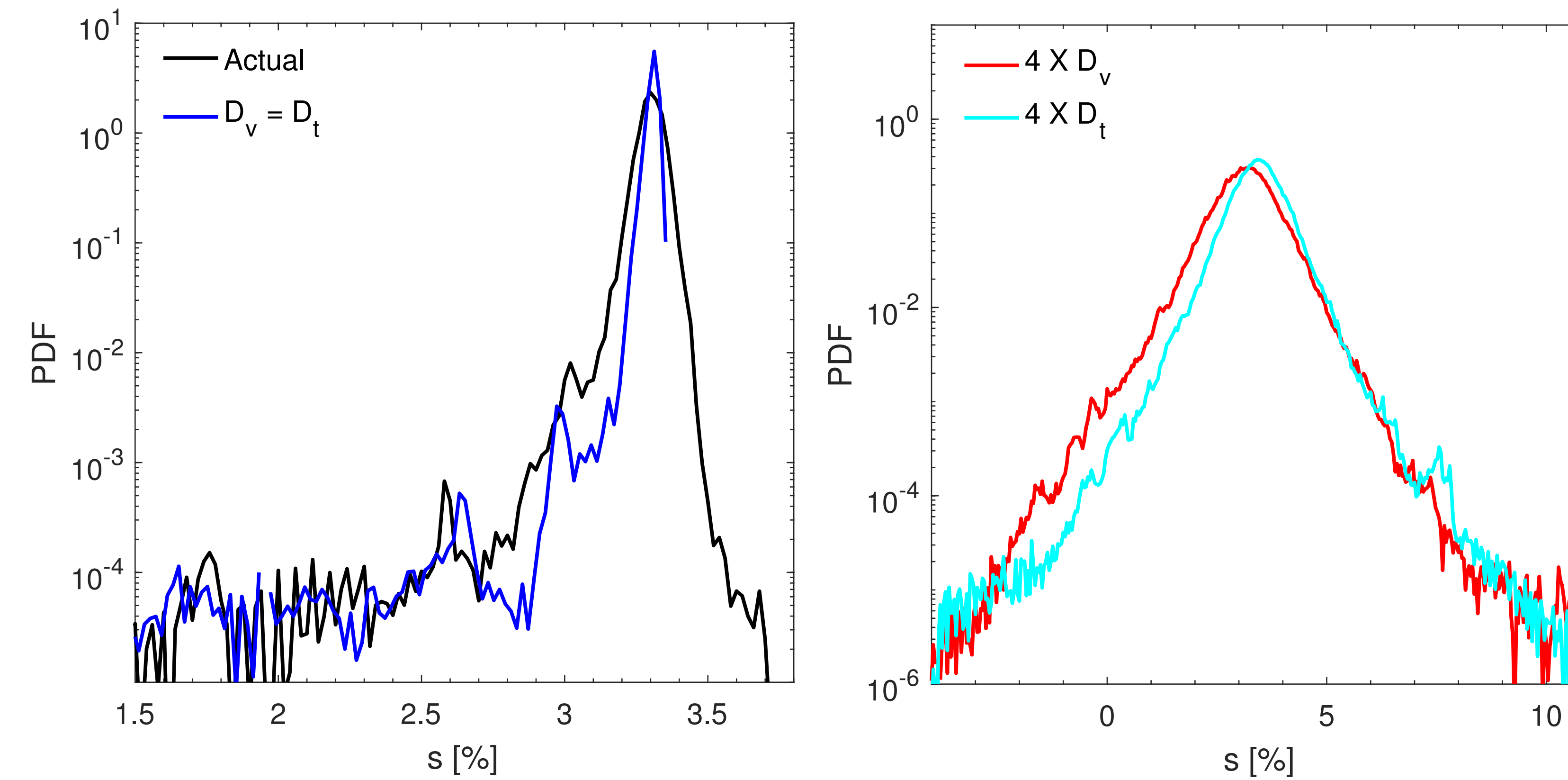


Figure 2: Sample PDFs of supersaturation near the domain center for the different diffusivity cases (8 K applied temperature difference).

## Scaling Analysis

### Moisture flux:

$$Sh \propto Sc^{1/2} Ra_{moist}^{1/3} |Pr \sim 1| \quad Sh \propto Sc^{1/2} Pr^{-1/3} Ra_{moist}^{1/3} |Pr \ll 1|$$

$Sh$  : Sherwood Number;  $Pr$  : Prandtl Number;  $Sc$  : Schmidt Number

### Supersaturation Fluctuations:

$$\sigma_s^2 \approx S^2 \left[ \left( \frac{\sigma_{e_v}}{\bar{e}_v} \right)^2 + \zeta^2 \left( \frac{\sigma_T}{\bar{T}} \right)^2 - 2\zeta \frac{\overline{T' e_v'}}{\bar{T} \bar{e}_v} \right]$$

$$\left( \frac{\sigma_s}{S} \right)^2 \sim \xi^2 \left[ 1 - \frac{1}{S} \left( \frac{Pr}{Sc} \right)^{1/2} \right]^2 Pr^{-2} (1 + \sqrt{Pr})^{-1} Ra_{moist}^{5/3} \left( \frac{z}{H} \right)^{-1}$$

$\sigma_T$ : temperature STD;  $\sigma_{qv}$ : water-vapor STD;  $z$ : vertical position;  $H$ : domain height;  $\xi \propto H^{-3}$

$\Delta T$ : applied temperature difference;  $\Delta q_v$ : applied water vapor mixing-ratio difference

$\nu$ : kinematic viscosity;  $D_t$ : thermal diffusivity;  $D_v$ : water vapor diffusivity

## Supersaturation Fluctuations in Bulk: Contributions from Both Scalars

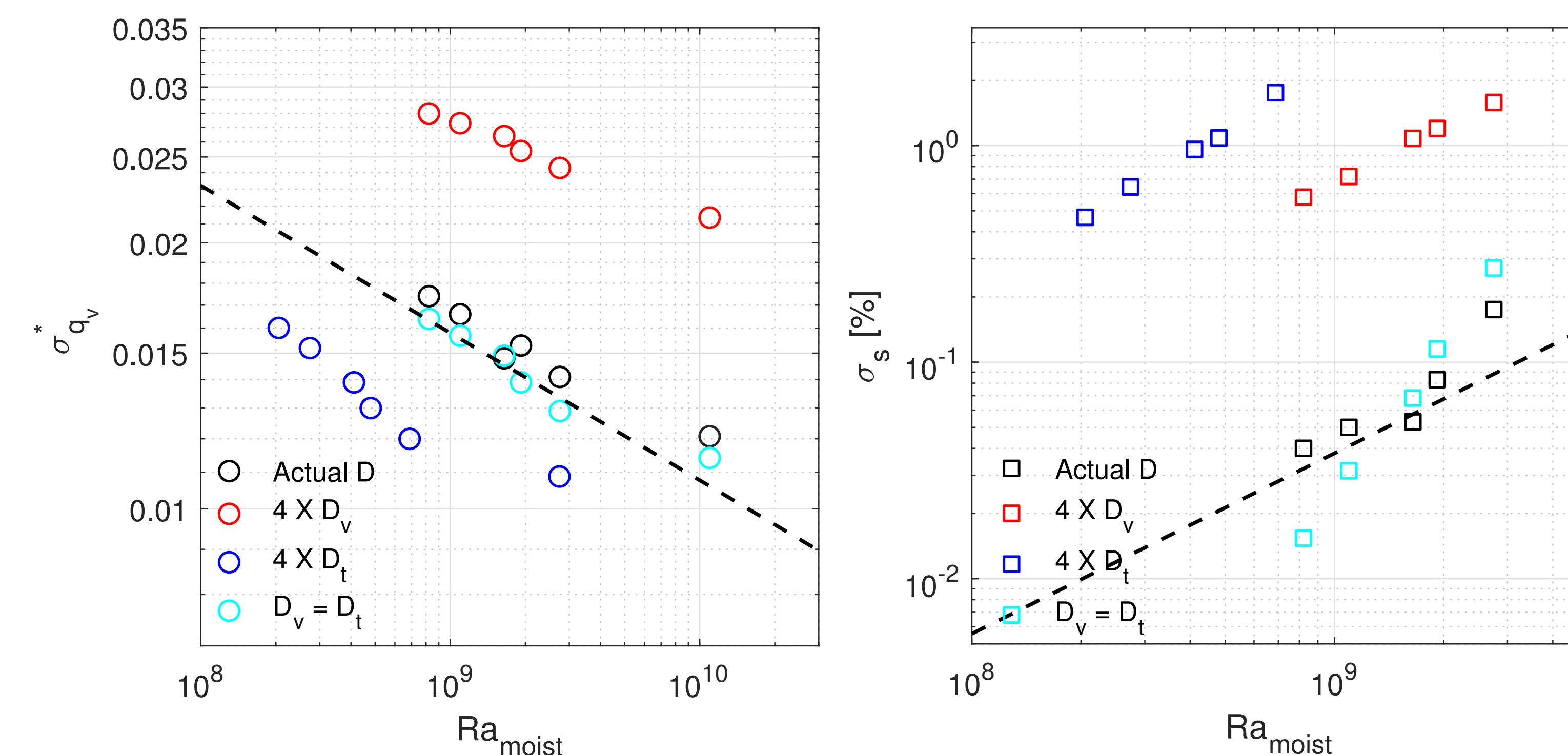


Figure 3: STDs of normalized water vapor mixing-ratio (**left**) and supersaturation fluctuation (**right**) at the domain center versus  $Ra_{moist}$ , and their comparison with scaling relations (dash-line)  $Ra_{moist}^{-1/6}$  and  $Ra_{moist}^{5/6}$ .

## Mixing Diagram

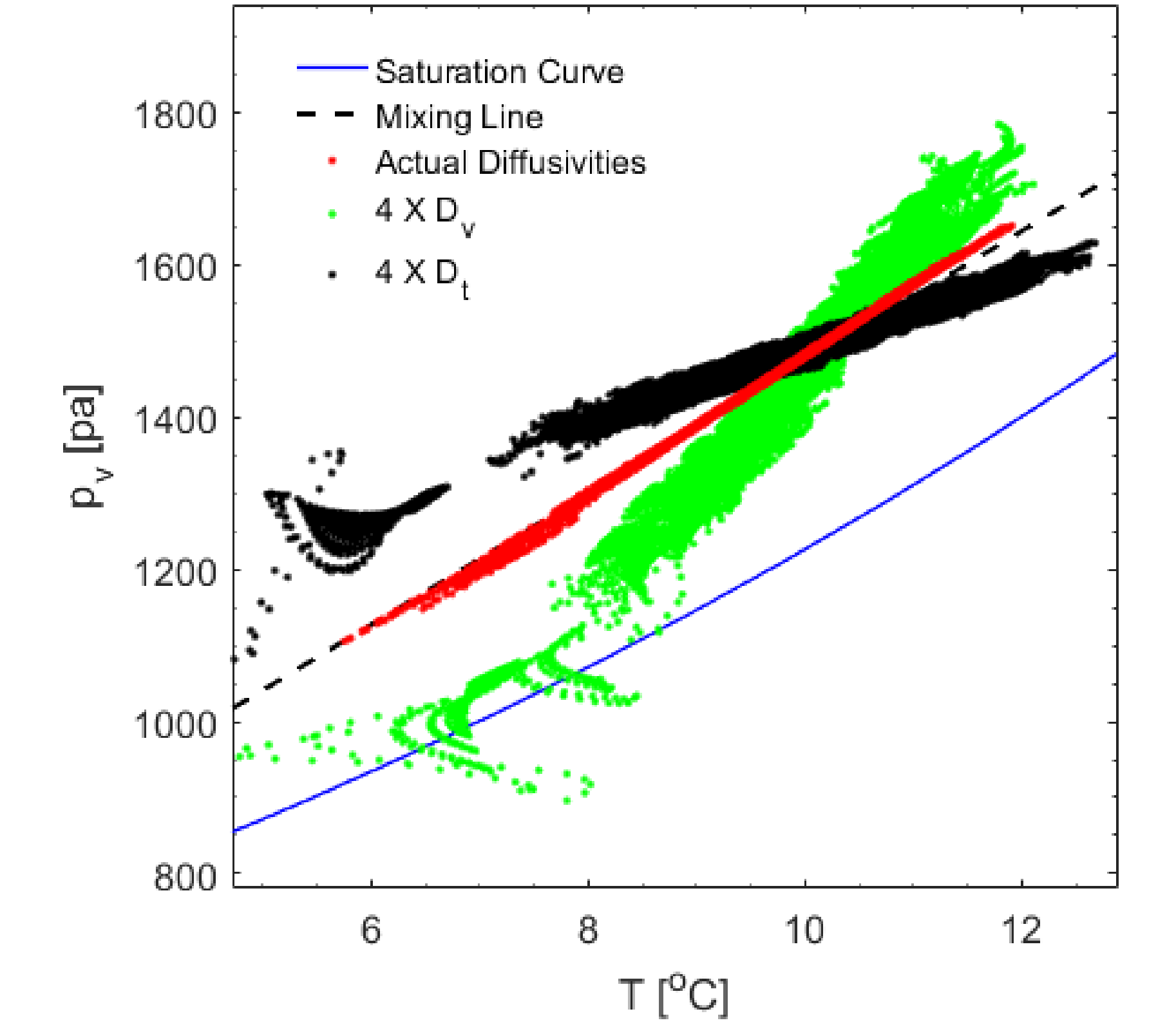


Figure 4: Mixing diagram for different diffusivity cases at 20K applied temperature difference.

## Conclusion

- Scaling relations for heat and moisture fluxes are obtained as a function of  $Ra_{moist}$ ,  $Pr$ , and  $Sc$ .
- In the bulk fluid,  $\sigma_T^*$  and  $\sigma_{qv}^*$  both follow a  $Ra_{moist}^{-1/6}$  scaling relation. Moreover, the magnitude of scalar fluctuations increases with an increase in the respective scalar diffusivity.
- PDFs of supersaturation become broader with an increase in absolute value of diffusivity difference. Also, PDFs are slightly negatively skewed for cases with low diffusivity difference, unlike the  $T$  and  $q_v$  PDFs.
- Both, scaling and numerical output suggests:  $\sigma_s^2 \propto Ra_{moist}^{5/3}/H^6$ .
- The analysis of numerical output shows similar order contributions to the supersaturation variance from both scalar variance and covariance.
- Distribution of points in a pressure-temperature mixing diagram deviate from the classical mixing line for isobaric mixing, when  $D_v \neq D_t$ .

## References

- [1] Chandrakar *et al.* *Proc. Natl. Acad. Sci. (USA)*, 113(50).
- [2] James W Deardorff. *J. Atmos. Sci.*, 27(8):1211–1213, 1970.
- [3] Douglas K Lilly. *Quart. J. Roy. Meteor. Soc.*, 94(401):292–309, 1968.
- [4] Kerry A Emanuel. Oxford University Press, 1994.
- [5] Niedermeier *et al.* *Phys. Rev. Fluids*, 3(8):083501, 2018.
- [6] Wunsch *et al.* *J. Fluid Mech.*, 528:173–205, 2005.

## Acknowledgements

This work was supported by National Science Foundation Grant AGS-1754244 and by the NASA Earth and Space Science Fellowship Program.